Energy and Thermofluids Engineering

Available at https://asps-journals.com

Effects of Asymmetric Channel on the Convective Heat Transfer: A Computational Study

Abu Hamja[1], Md. Tofazzal Hossain[1], Nahian Jalil Shubho[1], Tanzil Islam[1], Mohammad Rejaul Haque[1]

[1]*Department of Mechanical and Production Engineering (MPE), Ahsanullah University of Science and Technology (AUST), Dhaka-1208, Bangladesh*

Received August 31, 2022
Revised January 21, 2023
Accepted February 02, 2023
Published online: February 13, 2023

Keywords
Sinusoidal Channels
Symmetric Channels
Asymmetric Channels
Aspect Ratio
Heat Transfer
Heat Exchangers

Abstract: In the fields of engineering, especially in the heat transfer area, the contribution of the fluid flows through different channels is remarkable. Among the different available shapes in the channel, the sinusoidal wavy channels are considered more efficient in the heat transfer areas such as cooling of electronic devices, boilers, biomedical applications, etc., due to their increased recirculation capability of mixing the flowing fluids - which increases the heat transfer performance, consequently. The optimization of channel design and modelling has been an engineering problem in recent years. In this research, flat, symmetric sinusoidal, and asymmetric sinusoidal channels were designed - using ANSYS 2020 - to investigate the effects of channel shape, amplitude, and aspect ratio of sinusoidal wavy walls on the overall heat transfer performance. Several designs have been considered in the present study at different Reynolds numbers and different aspect ratios, keeping the wall temperature as constant. The results of this study exhibit that at an aspect ratio of 0.4, the asymmetric channel shows the highest heat transfer effect due to increased recirculation tendency.

1. INTRODUCTION

Researching ways to improve the rate of heat transfer in heat exchangers has become very necessary and important in most engineering applications in order to make the heat exchangers smaller and better heat transfer(Ahmed et al., 2014; Kenyu Oyakawa, Takao Shinzato, 1989; Rush et al., 1999). In the field of thermal engineering, improving performance is seen as the most important way to cut down on energy use (Rahman et al., 2013). The heat flux is strongly dependent on the flow pattern, and the flow patterns are dependent on several channel design variables. Most of the study has focused on improving heat transfer rates by altering the architecture of channels and flow patterns (Gong et al., 2011; Mellal et al., 2017; Ramgadia & Saha, 2012). As a result, the enhanced fluid mixing propensity in wavy channels makes them a viable alternative to conventional channels (i.e., flat channels) for improving heat exchanger thermal performance. By improving the thermophysical qualities (such as thermal conductivity) of flowing fluids, heat transfer rate can be speeded up. Nanoparticles may be added to the working fluids for improving the thermal performance of the heat exchanger (Ahmed et al., 2014). The sinusoidal wave amplitude, aspect ratio, and symmetricity can be used as design optimization parameters which can accelerate the thermal performance of the channels by inducing the higher recirculation effects on the thermal fluids.

A numerical analysis of the heat transfer rate in a sinusoidal wavy channel was performed(Wang & Chen, 2005). In their study, the authors investigated the effects of wavy geometry, Reynolds number (Re), and Prandtl number (Pr) on the skin-friction and Nusselt number by

✉Corresponding author. E-mail address: abuhamja.mpe@aust.edu

ENERGY AND THERMOFLUIDS ENGINEERING | ETE | ISSN2716-8026 (PRINT)
Available online at https://asps-journals.com/index.php/ete
https://doi.org/10.38208/ete.v2.462

employing a spline alternating-direction implicit approach and a simple coordinate transformation method. Nusselt number and skin-friction coefficient amplitudes grow with increasing Reynolds number and amplitude–wavelength ratio, according to their findings. When the amplitude wavelength ratio is sufficiently large, the corrugated channel is observed to be an efficient heat transfer device, particularly at higher Reynolds numbers, even if the heat transfer improvement is not substantial at lower amplitude wavelength ratios. An unstable laminar flow of a Newtonian fluid with sinusoidal walls has been studied using computational models(Grant Mills et al., 2014). The authors conducted their experiment at a constant pressure gradient and discovered two forms of unstable flows in a sinusoidal channel. According to their findings, channel furrow vortices are ejected downstream when their amplitude is relatively minor in comparison to that of the wavy walls. Vortices stay within the furrows and display periodic oscillations and topological changes when the wall wave amplitude is large enough to cause them to alter their shape. For building laminar heat/mass exchangers with unsteady flows, the optimal wall period and amplitude was determined that leads to an unsteady flow at the smallest pressure gradient.

Experimental research was conducted (Nishimura, 1995) in a serpentine and a converging-diverging channel with sinusoidal wavy walls, both of which have distinct geometry. In this experiment, the flow patterns and mass transfer rates were found to be influenced by the channel geometry. The fluid flow characteristics were described in terms of vortex dynamics, fluid mixing, and wall shear stress by numerical analysis and flow visualizations. At low Strouhal numbers, the serpentine channel outperforms the converging and diverging channels in terms of mass transfer and pumping power, the asymmetric channel is superior to the symmetric channel. A 2-D numerical analysis was accomplished of a fully developed flow and heat transfer through a sinusoidal wavy channel at horizontal conditions (Ramgadia & Saha, 2013). In their study, the finite volume method was used to solve the energy and Navier–Stokes equations. The authors have made several attempts to predict the influence that the stream-wise domain length, which is an integer multiple of the periodic domain length, would have an effect on the flow and heat transfer characteristics. The flow and heat transfer properties are shown to not affect the length of the periodic domain, thereby showing that geometric and flow periodicity is the same. The authors found that the transient flow with higher mixing between the core and relatively close fluids enhances the rate of heat transfer even when heat transfer coefficients are modest for steady flow. An Al_2O_3–water nanofluid flow in a sinusoidal-wavy channel has been numerically explored (Ahmed et al., 2014). Four unique phase shifts of 0°, 45°, 90°, and 180° were studied in a sine wave with a Reynolds number range of 100 – 800 and nanoparticle volume fractions of 0–5%. Flow and temperature contours, skin friction coefficient, local Nusselt number, thermal-hydraulic performance factor, and pressure drop have all been investigated in their research by varying phase shift, nanoparticle volume fraction, and Reynolds number. Over a wide range of Reynolds numbers and nanoparticle volume fractions, they found that a 0-degree phase shift channel provided the best performance. Several numerical research have accomplished on a fully developed laminar forced convection in sinusoidal corrugated plate channels with constant boundary temperature and constant single-phase flow properties (Hossain & Saha, 2021; Metwally & Manglik, 2004; Saha & Hossain, 2021). The authors obtained the numerical results using the control volume finite difference method for a wide range of flow regimes and aspect ratios (γ). They have found that no-swirl flows behave quite similarly to fully developed straight-duct flows without cross-stream disturbance in this regime. Flow separation and reattachment in the corrugation trenches produce crosswise swirling cells that develop spatially with Re and γ in the swirl regime. The shift to this regime is dependent on Re and γ as well during flow separation and reattachment. Depending on γ, Re, and Pr, the mixing created by these self-sustained transverse vortices improves heat transmission dramatically with a tiny friction factor cost.

Though numerous research works have been conducted in existing literature, limited research is available to investigate the effects of asymmetry of channels on heat transfer. Hence, the present work is an attempt to improve the heat transfer performance for channel flow. In this study, we focused on the effects of asymmetric geometrical parameters of channels on heat transfer. To perform this computational fluid dynamics (CFD) analysis, the commercial academic software ANSYS 2020 has been used. Three different types of channel geometries, such as flat, symmetric sinusoidal, and asymmetric sinusoidal, were designed to investigate the

effects of channel shape, amplitude, and aspect ratio of sinusoidal wavy walls on the overall heat transfer aiming two prime objectives. Firstly, maintaining the area and temperature difference as constant, the heat transmission is to be enhanced. Secondly, to maintain the heat transmission and temperature differential as constant, the area has to be lowered. Researchers have recommended many forms of channels, such as sinusoidal channels, twisted channels, etc., for boosting the performance of heat transfer in laminar fluid flow.

2. MATERIALS AND METHODS

As shown in Fig. 1(a) and Fig. 1(b), the present considered models are symmetric and asymmetric channels, respectively, with 10 mm pipe length and 1.25 mm width. The amplitude of the sine wave for both cases was kept constant at 0.625 mm. The simulations have been performed at a constant Reynolds number of 600. Air has been taken as the working fluid. During the cooling analysis, the inlet air and channel wall temperatures were kept at 350 K and 300 K, respectively. And during heating analysis, the inlet air and channel wall temperatures were 300 K and 350 K, respectively. Both cases were performed assuming the flow as the steady and incompressible. Table 1 shows the summary of the geometry parameters and boundary conditions that have been used in the computation.

Table 1: Geometrical parameters and boundary conditions.

Items	Dimensions and Descriptions	
Cases	Symmetric Channel	Asymmetric Channel
Channel Parameters:		
Total pipe length (mm)	10	10
Pipe width (mm)	1.25	1.25
Boundary Conditions:		
Cooling Analysis:		
Inlet Air Temperature, (K)	350	350
Channel Wall Temperature, (K)	300	300
Heating Analysis:		
Inlet Air Temperature, (K)	300	300
Channel Wall Temperature, (K)	350	350

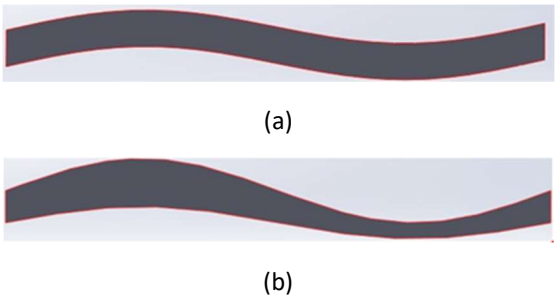

(a)

(b)

Fig. 1(a) Symmetric channel model, and (b) Asymmetric channel model.

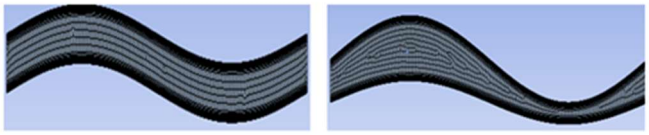

(a) (b)

Fig. 2 Meshed geometry with 2D quadrilateral grid elements of (a) symmetric model, and (b) asymmetric model.

MESH GENERATION

The generated mesh of the model is depicted in Fig. 2. To ensure the accuracy of the obtained results, the grid system and structure are crucial. The various interface zones have grown a much finer mesh. The overall structure of the model has been meshed using the Patch-confirming tetrahedron grid elements. Tetrahedral grid elements are ideal for meshing computational domains with complicated shapes (Nemati Taher et al., 2012). Hence, in this case, we used a tetrahedral mesh because of its adaptability and the simplicity of automated mesh production.

3. GRID INDEPENDENCY TEST

Both the numerical analysis and the validation process are greatly influenced by the quality of the grid element structure. As a consequence, significant considerations for grid independence are required to assure the credibility of the numerical findings. The grid-independent test was computed using various node or element sizes of the domain. For nodes 376251 to 476451, there was very little fluctuation in the 'maximum velocity', as shown in Fig 3. The optimal element size for this investigation was 376251, which was selected because the results are almost same for subsequent number of meshing.

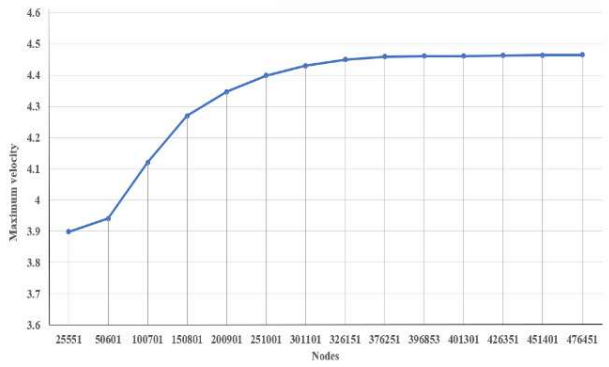

Fig. 3 The grid system's mesh independence test for numerical solutions

4. MATHEMATICAL MODELING

Computer simulations are helpful for learning about the inner workings of even the most complex systems. These types of simulations construct an overall model of the system by combining digital representations of its constituent parts. It's important to know what each part does and that it works with that particular application. It is based on the simulated circumstances of fluid mechanics and heat exchange. Hence, corresponding governing equations of flow characteristics have been used. The turbulent flow was modelled using the RNG k– ε turbulence model. Because molecular viscosity is considered to be minimal in the formulation of the k– ε model and the flow is entirely turbulent, and the k– ε model can only be used for fully turbulent flows (ANSYS, 2021). When compared to other RNG models, the k– ε model uses less memory and takes less time to calculate. It is also critical to use this model to accurately anticipate the heat transfer output in the areas next to the wall.

Following the grid independence and material selection, the model went through the final analysis in ANSYS CFD simulation. The boundary conditions as shown in Table 1, were applied using the appropriate k– ε model and iterative parametric values. The fluid properties were chosen from built-in water properties in ANSYS.

In the ANSYS CFD calculations, the following mathematical equations for energy, momentum, continuity, k, and ε were used considering steady and incompressible flow:

Continuity equation:
$$\nabla \cdot (\rho u) = 0 \tag{1}$$

Momentum equation:
$$(\nabla \cdot u)\rho u = -\nabla p + \nabla \cdot \mu(\nabla u + (\nabla u)^T) \tag{2}$$

Energy equation:
$$\rho c_p u(\nabla T) = \nabla \cdot (K \nabla T) + \emptyset \tag{3}$$

Turbulent kinetic energy (Eq. (5)) and energy dissipation (Eq. (4)) have been used in this work to develop the conventional *k-ε* model.

$$\rho(u.\nabla)\varepsilon = \nabla \cdot \left[\left(\mu + \frac{\mu T}{\sigma \varepsilon}\right)\nabla \varepsilon\right] + C_{\varepsilon 1}\frac{\varepsilon}{k}P_k - C_{\varepsilon 1}\rho\frac{\varepsilon^2}{k}, \varepsilon = ep \tag{4}$$

$$\rho(u.\nabla)k = \nabla \cdot \left[\left(\mu + \frac{\mu T}{\sigma k}\right)\nabla k\right] + P_k - \rho\varepsilon \tag{5}$$

Where the production term is:
$$P_k = \mu_T[\nabla u : (\nabla u + (\nabla u)^T)] \tag{6}$$

The turbulent viscosity is:
$$\mu_t = \rho C_\mu \frac{k^2}{\varepsilon} \tag{7}$$

The conventional turbulence *k-ε* model's experimental constants are as follows:

$$C_\mu = 0.09, C_{\varepsilon 1} = 1.44, C_{\varepsilon 2} = 1.92, \sigma_k = 1, \sigma_e = 1.3$$

Using Eq. 8 and the pressure differential throughout the channel length (*L*), the friction factor (*f*) is computed.

$$f = \frac{2}{(L/D_h)}\frac{\Delta P}{\rho U^2} \tag{8}$$

Eq. 9 is used to determine how much convection and conductive heat transfer occur in the same layer of heat transfer, defining the local Nusselt number.

$$Nu_{(x)} = \frac{h_X D_x}{K_F} \tag{9}$$

The area integral of Eq. 9 may be used to get the total Nusselt number (Eq. 10).

$$Nu = \frac{1}{A}\int Nu_{(x)}\, \partial A \tag{10}$$

In addition, to address the channel's geometrical effects, we used the aspect ratio (γ) as shown in Eq. (11), which means the ratio of the channel thickness at the inlet position and the single wavelength as seen in Fig. 4(a) and Fig. 4(b). In this simulation, the wave length is fixed for every design, but this aspect ratio has been varied from 0.1 to 1.

$$\gamma = \frac{2a}{\lambda} \tag{11}$$

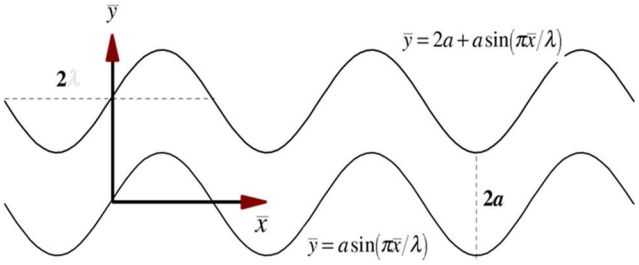

(a)

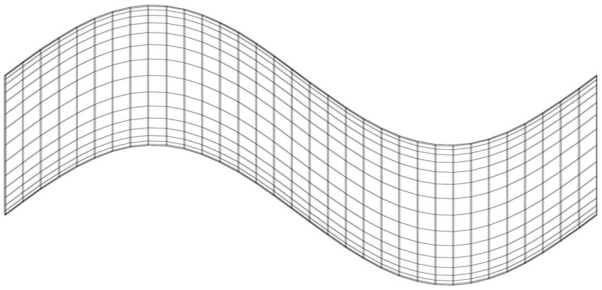

(b)

Fig. 4 In-phase sinusoidally corrugated parallel-plate channel: (a) physical domain, and (b) computational domain

5. RESULTS AND DISCUSSION

To validate the numerical scheme, tests of the overall Nusselt number, Nu (Eq. (12)) at different Reynolds numbers, Re (Eq. (13)) are performed for a fixed value of Prandtl number of 5. – A Prandtl number higher than unity ensures higher momentum transferred compared to thermal diffusion resulting higher heat transfer rate. Moreover, these results have been compared with the results of Heidary & Kermani (Fig. 5) (Heidary & Kermani, 2010). As illustrated in Fig.5, the current research findings are compared to those of Heidary and Kermani for various Reynolds numbers. In their study, the Nu number was found to be varied with the Re at fixed wave amplitude of 0.2. On the other hand, in this study, the Nu number has been derived for the asymmetric sinusoidal channel at a constant aspect ratio of 0.4. It's clear from this study that both of the cases have the same general tendency, and the variance can be traced back to certain losses.

$$Nu = 0.36\mathrm{Re}^{0.55}\,\mathrm{Pr}^{0.33}\left(\frac{\mu_t}{\mu_w}\right)^{0.14} \quad (12)$$

$$Re = \frac{\rho\, v\, D}{\mu} \quad (13)$$

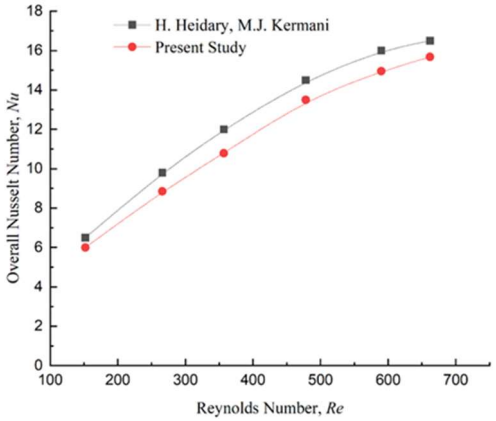

Fig. 5 Overall Nusselt number for different Reynolds numbers

6. COOLING PROCESS

Fig. 6 (a-g) shows the channel wavelength variation at different Reynolds numbers as a result of the cooling process. As it is seen in these figures, increasing the Re number causes an increase in the mean outlet temperature for each channel. Nonetheless, in the asymmetry channel, the average outlet temperature is lower than in the flat or symmetric channels because of more intense fluid contact. Using an asymmetry channel with an aspect ratio of 0.125 and a Re of 100 as shown in Fig. 6(a), the mean temperature difference between the inlet and outlet air is 43.68 K. It is also worth noting that, in the wide area (x = 0.005 mm), the temperature of the asymmetry channel is higher than that of the symmetry, while in the narrow region (x = 0.015 mm), this temperature is lower.

Overall Nusselt numbers for all channels are increasing as a result of increased aspect ratio and Reynolds number, as seen in Figs.7(a) and 7(b). It has been found that the highest Nusselt number of 17.5 may be achieved when the Re is 100. The asymmetries have higher Nusselt numbers compared to symmetrical ones. However, for all Reynolds numbers, the asymmetries in the gamma-0.4 range have the highest Nusselt numbers. Overall Nusselt number for $\gamma = 0.4$ asymmetry channel is respectively, 37.6%, 47.1%, 58.0%, 67.8%, 74.3%, 92.6%, 85.4% higher than the flat channel, and 13.6%, 17.0%, 19.8%, 19.2%, 22.7%, 22.2% higher than the symmetry channel having the same aspect ratio when the Re numbers were 100, 200, 300, 400, 500, 600, and 700, respectively. High pumping power is needed to move fluid through a high aspect ratio channel because of the increased pressure drop caused by the higher aspect ratio. Higher aspect ratios have lower Nusselt numbers than smaller aspect ratios.

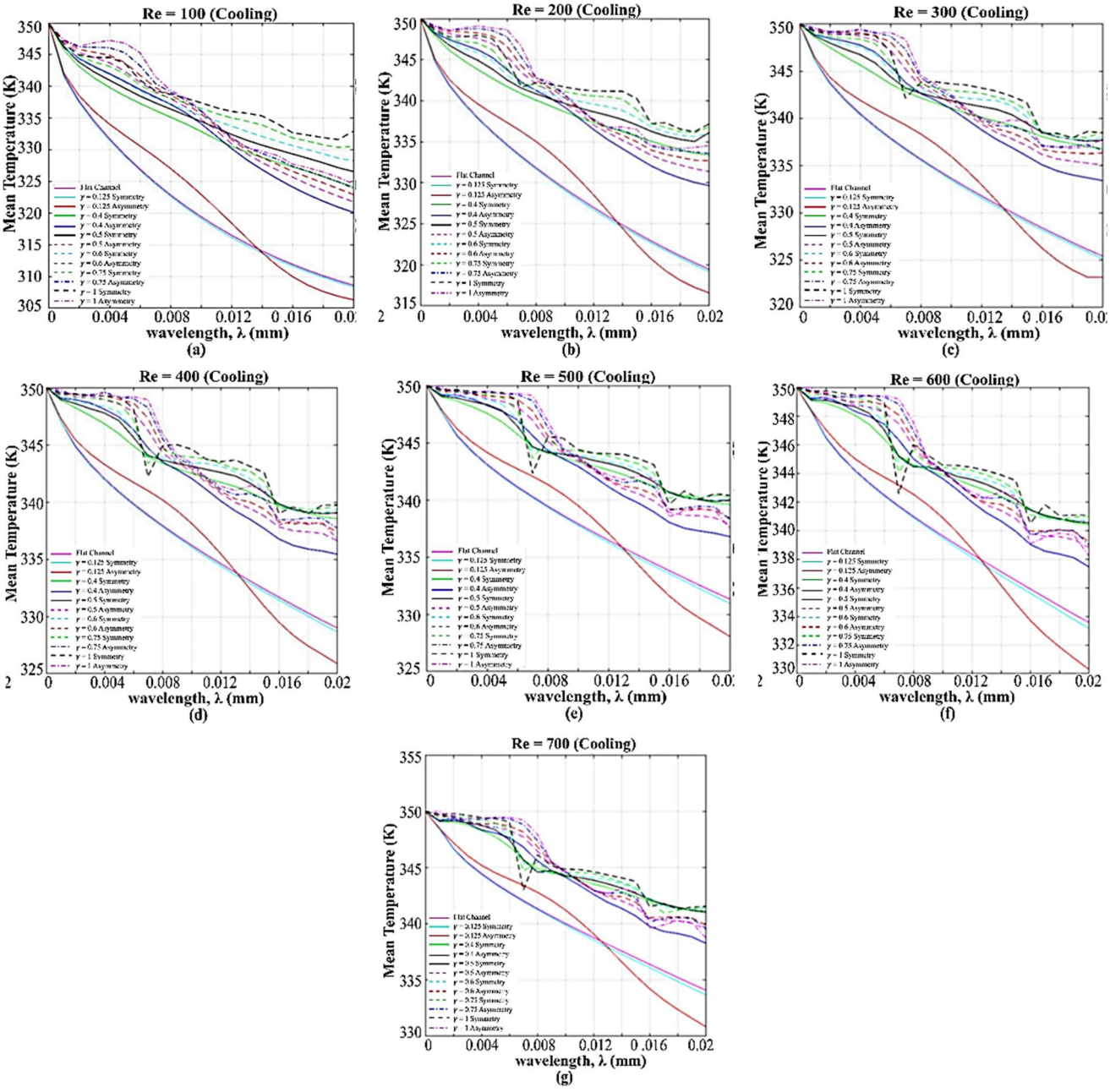

Fig.6 Temperature variation along the channel location for cooling processes at different Reynolds numbers of **a)** Re=100, **b)** Re=200, **c)** Re=300, **d)** Re=400, **e)** Re=500, **f)** Re=600. And **g)** Re=700.

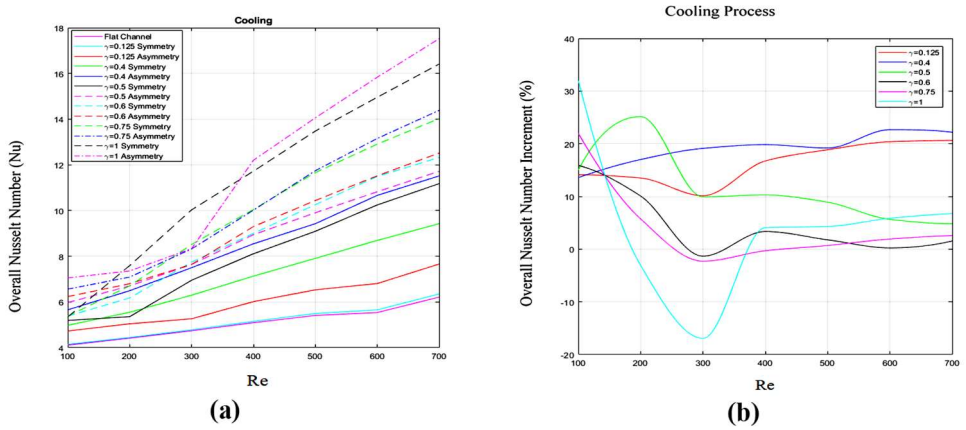

Fig. 7 (a) Nu vs Re for cooling and **(b)** Overall Nu number increment % vs Re for cooling

7. HEATING PROCESS

When the Re =100, the highest heating temperature is 343.68K, as shown in Fig. 8 (a-g). This is achieved by utilizing an asymmetry channel with an aspect ratio of 0.125. Gamma 1 -asymmetrical channel has a higher Nusselt number than any other symmetry or flat channel, although Re number (Re=700) is different in the cooling operation. For example, the asymmetry channel has a lower mean temperature in the wide region, while it has a greater mean temperature in the small portion of the asymmetry channel. As with the other asymmetric and flat channels, the aspect ratio of 0.4 channel performs better. Overall Nusselt number (Fig 8 (a-b)) for this channel is respectively 37.5%, 49.3%, 64.6%, 77.4%, 82.1%, 91.8%, 85% higher than flat channel and 13.6%, 18.8%, 23.9%, 26.7%, 24.6%, 22.2%, 22.2% higher than the same aspect ratio's symmetry channel.

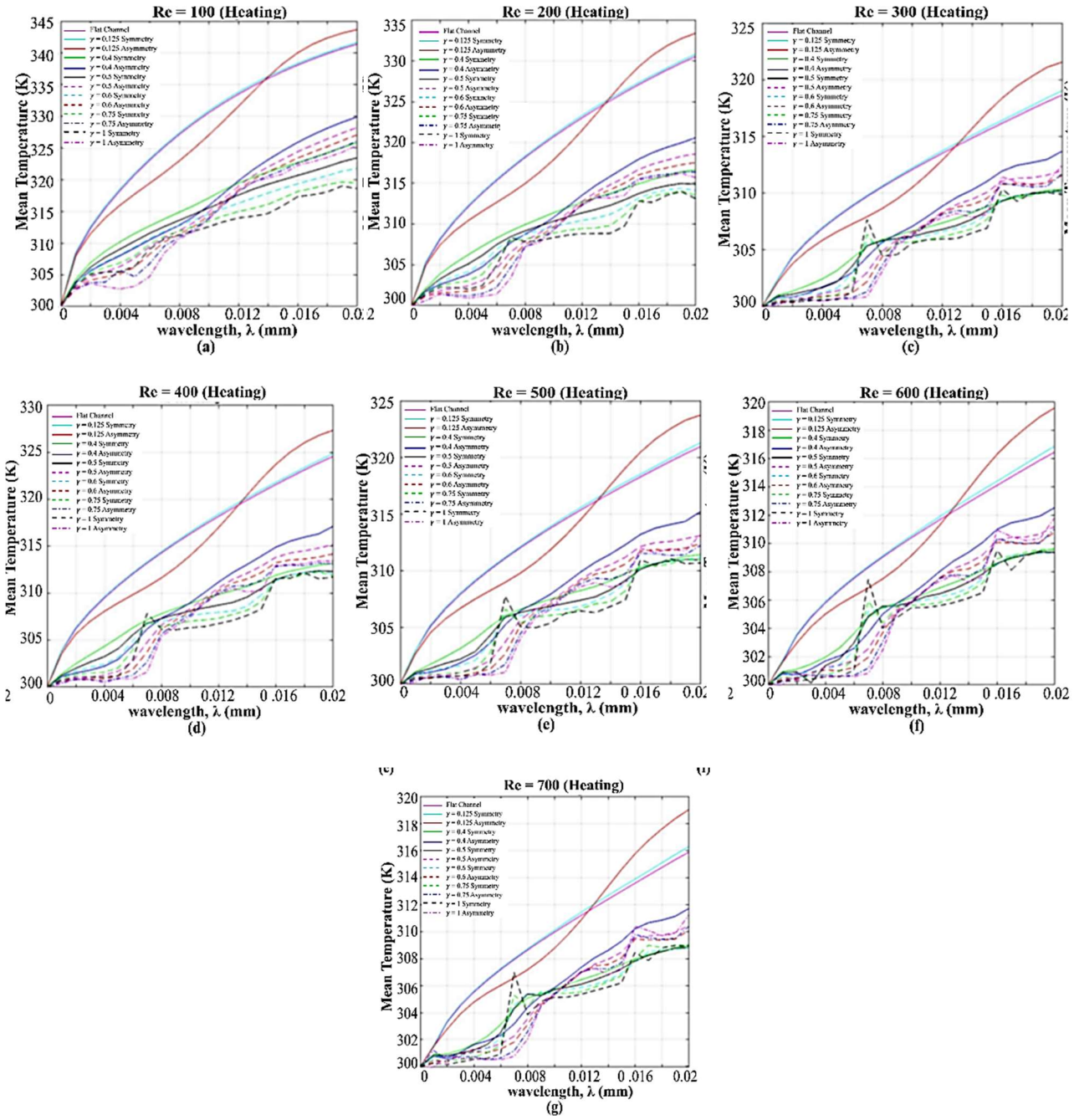

Fig. 8 Temperature variation along the channel location for heating processes at different Reynolds Numbers: **a)** Re=100, **b)** Re=200, **c)** Re=300, **d)** Re=400, **e)** Re=500, **f)** Re=600, and **g)** Re=700

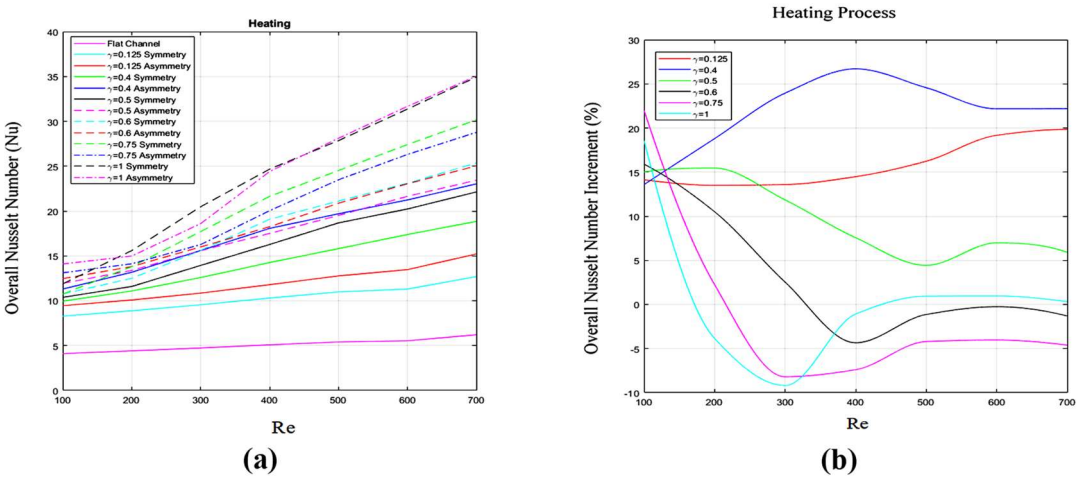

Fig. 9 (a) Nu vs Re for heating and **(b)** Overall Nu number increment % vs Re for heating

Fig. 10 depicts the asymmetric channel's temperature profile at an aspect ratio of 0.4. Flow velocity and temperature throughout the channel were seen in the red zone, indicating that the inlet air temperature was 350K (as determined by the boundary condition). The temperature was consistent with the fluid's velocity and temperature as it passed through the channel. Fluid was unable to get through the wall at the crest of the vortex, and it appears blue at the peak. As a result, they have a better heat transfer.

At varying Reynold's numbers, the asymmetric channel's velocity contour is shown in Fig. 11. When the air enters the inlet, it travels in a straight line, but when it strikes the pipe's surface, the velocity drops, and the colour turns blue. The fluid is moving normally through the channel, as indicated by the green colour. The red colour indicates that the channel area has contracted, indicating a decrease in fluid pressure and an increase in fluid velocity.

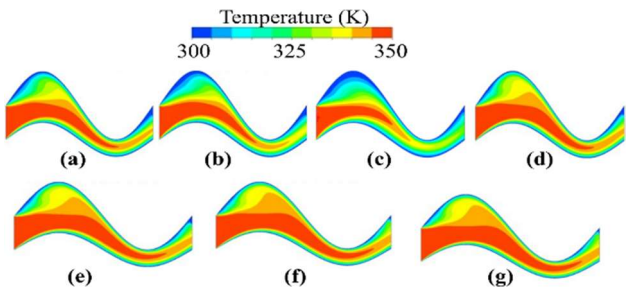

Fig. 10 Temperature profiles for asymmetry channel (γ = 0.4) at different values of Reynolds number a) Re=100, b) Re=200, c) Re=300, d) Re=400, e) Re=500, f) Re=600, and g) Re=700

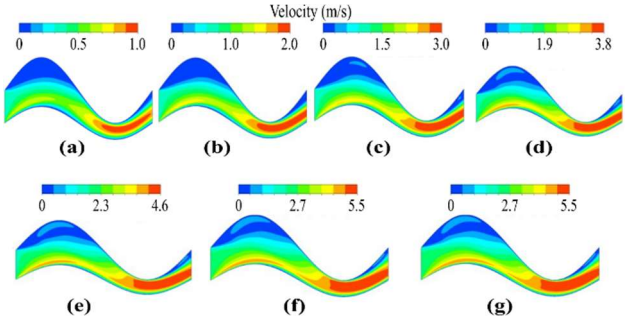

Fig. 11 Velocity profiles for asymmetry channel (γ = 0.4) at different Reynolds numbers a) Re=100, b) Re=200, c) Re=300, d) Re=400, e) Re=500, f) Re=600, and g) Re=700

Asymmetric channel velocity streamlines are shown in Fig. 12 for various Reynold's numbers. It demonstrates that when air enters the inlet, it travels in a straight line, but as it strikes the pipe's surface, the velocity drops, and the outlet vortex can be seen. The red colour indicates that the channel area has contracted, indicating a decrease in fluid pressure and an increase in fluid velocity.

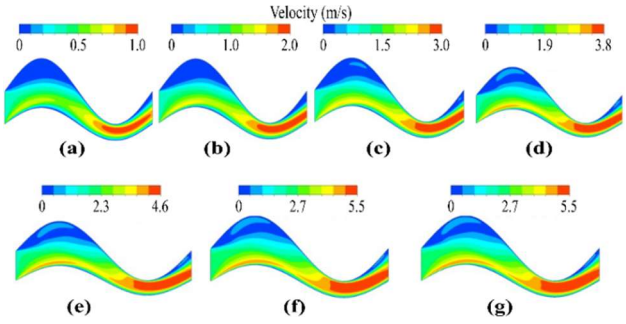

Fig. 12 Streamline profiles for asymmetry channel (γ = 0.4) at different Reynolds number; a) Re=100, b) Re=200, c) Re=300, d) Re=400, e) Re=500, f) Re=600, and g) Re=700

8. Conclusion

In this research, numerical simulations of symmetric and asymmetric channels have been carried out to study the impact of channel geometry, amplitude, and the aspect ratio of sinusoidal wavy walls on total heat transfer performance. The temperature change in the channel configuration during cooling and heating operations has been studied at various Reynolds numbers. The aspect ratio of 0.4 shows the optimal results for both symmetric and asymmetrical channels. The outlet temperature of the asymmetry channel is lower than the flat and symmetry channels during cooling because of fluid mixing in the asymmetry channel. The mean temperature in an asymmetry channel is lower than in asymmetry channel or the flat channel. When heating, the vast area of the asymmetry channel has a lower mean temperature than the symmetry and flat channels, while the tiny area has a higher mean temperature than the symmetry and flat channels. Overall Nusselt number for cooling is highest for asymmetry channel having a γ value of 0.4 than for any other symmetrical or asymmetrical channels. While heating, the γ of 0.4 asymmetries surpasses the other symmetrical and flat channels by a significant margin.

9. CONFLICTS OF INTEREST

The authors of this research work have declared and confirmed that there are no conflicts of interest linked to this piece of research.

Acknowledgments

The authors would like to acknowledge the simulation lab of the Mechanical and Production engineering department of Ahsanullah University of Science and Technology.

Disclosures

Free Access to this article is sponsored by SARL ALPHA CRISTO INDUSTRIAL.

Nomenclature

ρ	Density [kg/m3]
t	Time [s]
∅	Heat generation rate [W/m2]
∇	Divergence [1/s]
v	Velocity [m/s]
P	Static pressure [Pa]
τ	Stress tensor [Pa]
ρg	Gravitational Force [N]
F	Force [N]
γ	Aspect ratio [-]
λ	Wavelength [m]
Cp	Specificheat [J/kg K]
hs	Convective heattransfer coefficient [W/m2K]
k	Turbulent kineticenergy [J/kg]
Nu	Nusseltnumber
μ_t	Turbulent viscosity [Pa.s]
ε	Energy dissipation [m2/s3]
f	Friction factor [-]
η	Thermal enhancement factor [-]
Re	Reynolds number

References

Ahmed, M. A., Yusoff, M. Z., Ng, K. C., & Shuaib, N. H. (2014). The effects of wavy-wall phase shift on thermal-hydraulic performance of Al2O3-water nanofluid flow in sinusoidal-wavy channel. *Case Studies in Thermal Engineering*, *4*, 153–165. https://doi.org/10.1016/j.csite.2014.09.005

ANSYS. (2021). *ANSYS Fluent Theory Guide* (No. 2021). Inc. (August 2021) 2600 Ansys Drive.

Cengel, Y. A. (1997). *Introduction to thermodynamics and heat transfer* (2nd ed.). McGraw-Hill.

Gong, L., Kota, K., Tao, W., & Joshi, Y. (2011). Parametric numerical study of flow and heat transfer in microchannels with wavy walls. *Journal of Heat Transfer*, *133*(5). https://doi.org/10.1115/1.4003284

Grant Mills, Z., Shah, T., Warey, A., Balestrino, S., & Alexeev, A. (2014). Onset of unsteady flow in wavy walled channels at low Reynolds number. *Physics of Fluids*, *26*(8). https://doi.org/10.1063/1.4892345

Heidary, H., & Kermani, M. J. (2010). Effect of nano-particles on forced convection in sinusoidal-wall channel. *International Communications in Heat and Mass Transfer*, *37*, 1520–1527. https://doi.org/10.1016/j.icheatmasstransfer.2010.08.018

Hossain, T., & Saha, B. (2021). *Optimization of Thermal Performance of a Segmental Baffle Shell and Tube Heat Exchanger under Different Baffle Spaces and Baffle Numbers : A Numerical Case Study Using CFD*. *3*(2), 1–15. https://doi.org/http://dx.doi.org/10.5281/zenodo.5526489

Kenyu Oyakawa, Takao Shinzato, I. M. (1989). The Effects of the Channel Width on Heat-Transfer Augmentation in a Sinusoidal Wave Channel. *JSME International Journal*, *32*(3), 403–410. https://doi.org/https://doi.org/10.1299/jsmeb1988.32.3_403

Mellal, M., Benzeguir, R., Sahel, D., & Ameur, H. (2017). Hydro-thermal shell-side performance evaluation of a shell and tube heat exchanger under different baffle arrangement and orientation. *International Journal of Thermal Sciences*, *121*,

138–149. https://doi.org/10.1016/j.ijthermalsci.2017.07.011

Metwally, H. M., & Manglik, R. M. (2004). Enhanced heat transfer due to curvature-induced lateral vortices in laminar flows in sinusoidal corrugated-plate channels. *International Journal of Heat and Mass Transfer*, *47*(10–11), 2283–2292. https://doi.org/10.1016/j.ijheatmasstransfer.2003.11.019

Nemati Taher, F., Zeyninejad Movassag, S., Razmi, K., & Tasouji Azar, R. (2012). Baffle space impact on the performance of helical baffle shell and tube heat exchangers. *Applied Thermal Engineering*, *44*, 143–149. https://doi.org/10.1016/j.applthermaleng.2012.03.042

Nishimura, T. (1995). Oscillatory flow and mass transfer within asymmetric and symmetric channels with sinusoidal wavy walls. *Heat and Mass Transfer*, *30*(4), 269–278. https://doi.org/10.1007/BF01602773

Rahman, M., Hamja, A., & Chowdhury, H. N. (2013). PHASE CHANGE MATERIALS: Characteristics and Encapsulation. *International Conference on Mechanical Engineering and Renewable Energy 2013 (ICMERE2013) 24- 27 December 2013, Chittagong, Bangladesh*, *December 2013*.

Ramgadia, A. G., & Saha, A. K. (2012). Large Eddy simulation of turbulent flow and heat transfer in a ribbed coolant passage. *Journal of Applied Mathematics*, *2012*. https://doi.org/10.1155/2012/246313

Ramgadia, A. G., & Saha, A. K. (2013). Numerical study of fully developed flow and heat transfer in a wavy passage. *International Journal of Thermal Sciences*, *67*, 152–166. https://doi.org/10.1016/j.ijthermalsci.2012.12.005

Rush, T. A., Newell, T. A., & Jacobi, A. M. (1999). An experimental study of flow and heat transfer in sinusoidal wavy passages. *International Journal of Heat and Mass Transfer*, *42*(9), 1541–1553. https://doi.org/10.1016/S0017-9310(98)00264-6

Saha, B., & Hossain, T. (2021). *Impact of Baffle Spaces and Baffle Numbers on Pressure Drop and Heat Transfer in a Shell and Tube Heat Exchanger : A CFD Analysis*. *October*, 1–14. https://doi.org/http://dx.doi.org/10.5281/zenodo.5554099

Wang, C. C., & Chen, C. K. (2005). Forced Convection in Micropolar Fluid Flow through a Wavy-Wall Channel. *Numerical Heat Transfer; Part A: Applications*, *48*(9), 879–900. https://doi.org/10.1080/10407780500226712